September 3, 2021

Over-expression Screen of Interferon-Stimulated Genes Identifies RARRES3 as a Restrictor of *Toxoplasma gondii* Infection

Nicholas Rinkenberger[a], Michael E. Abrams[b], Sumit K. Matta[a], John W. Schoggins[b], Neal M. Alto[b], David Sibley[a*]

[a]Department of Molecular Microbiology, Washington University in St. Louis, St. Louis, Missouri, USA

[b]Department of Microbiology, University of Texas Southwestern, Dallas, Texas, USA

Running title: *ISG screen for Toxoplasma inhibitors*

*Corresponding author: sibley@wustl.edu

Abstract

Toxoplasma gondii is an important human pathogen infecting an estimated 1 in 3 people worldwide. The cytokine interferon gamma (IFNγ) is induced during infection and is critical for restricting *T. gondii* growth in human cells. Growth restriction is presumed to be due to the induction interferon stimulated genes (ISGs) that are upregulated to protect the host from infection. Although there are hundreds of ISGs induced by IFNγ, their individual roles in restricting parasite growth in human cells remain somewhat elusive. To address this deficiency, we screened a library of 414 IFNγ induced ISGs to identify factors that impact *T. gondii* infection in human cells. In addition to IRF1, which likely acts through induction of numerous downstream genes, we identified RARRES3 as a single factor that restricts *T. gondii* infection by inducing premature egress of the parasite in multiple human cell lines. Overall, while we successfully identified a novel IFNγ induced factor restricting *T. gondii* infection, the limited number of ISGs capable of restricting *T. gondii* infection when individually expressed suggests that IFNγ mediated immunity to *T. gondii* infection is a complex, multifactorial process.

Key words: Intracellular parasite, egress, cell death, interferon gamma, growth restriction

Introduction

Toxoplasma gondii infection is common in humans, and while typically self-limiting in immunocompetent individuals, it can be severe in congenital toxoplasmosis and in immunodeficient individuals (1). Additionally, *T. gondii* is a leading cause of infectious retinochoroiditis (2). Eye disease is most prominent in Latin America and Africa with approximately one third of uveitis cases being attributed to ocular toxoplasmosis(3). Although mechanisms of immune control are well studied in the mouse, they are less well understood in humans with currently known mechanisms of restriction observed in a cell type dependent manner(4).

In response to pathogen infection, host cells express and secrete interferons (IFNs), which signal in an autocrine or paracrine manner through IFN receptors to induce factors designed to block infection. Interferons fall into three categories: type I (including IFNα and IFNβ), type II (IFNγ), and type III (IFNλ1-4). In general, receptors for type I and II IFN are ubiquitously expressed whereas type III IFN sensitivity is restricted to epithelial barriers. Conventionally, IFN signaling involves the induction of interferon stimulated genes (ISGs) involved in host defense via JAK-STAT mediated signaling (5-7). Although IFN upregulates expression of many genes, induction of ISGs is only semiconserved between cell types, with many ISGs being cell type dependent (7). Variability in ISG expression is perhaps due to the induction of noncanonical IFN signaling pathways that have been observed in a cell type dependent manner(8, 9). To identify and study the functions of this diverse set of genes, a wide variety of approaches have been utilized including ectopic overexpression, siRNA-mediated knockdown, and more recently CRISPR-Cas9 screening approaches(7). For the purpose of our study, several previous over-expression screens have been informative: an ectopic expression-based screen of type II IFN induced genes developed by Abrams et al., and the prior screen developed by Schoggins et al., which focused on type I IFN induced genes (10, 11). These screens utilized a lentiviral based expression cassette to express a curated library of commonly expressed ISGs in a one gene per well format. Abrams et al., successfully used this approach to identify novel ISGs which impact *Listeria monocytogenes* infection while the screen developed by Schoggins et al., has been used to identify many ISGs impacting a broad range of pathogens including both bacteria and viruses(10-13).

Interferon gamma (IFNγ) has been known since the 1980s to be expressed during *T. gondii* infection and to be critical for restricting infection in mice(14-16). IFNγ mediated restriction has been attributed to the expression of a group of interferon stimulated genes (ISGs) including immunity related GTPases (IRGs) and guanylate binding proteins (GBPs). IRGs and GBPs are recruited to the parasitophorous vacuole membrane (PVM) resulting in a loss of membrane integrity and parasite death(17, 18). As a defense, type I and II strains of *T. gondii* express the Ser/Thr kinase ROP18, which phosphorylates and inactivates IRG proteins to prevent PVM damage(19). Additionally, increased nitric oxide production due to induction of inducible nitric oxide synthase (iNOS) has also been shown to play a role in restricting *T. gondii* infection in mice *in vivo* and *in vitro*(20-22).

IFNγ is similarly important for *T. gondii* restriction in human cells *in vitro* and IFNγ expression has been shown to correlate with disease severity *in vivo*(23, 24). However, in contrast to the situation in mouse, the mechanisms underlying IFNγ mediated *T. gondii* restriction in humans tend to be cell-type specific. Humans possess one truncated IRG that likely lacks GTPase activity and only one nontruncated IRG that is not IFNγ or infection inducible(25). Hence, it is unlikely IRGs play a role in human resistance to *T. gondii* infection. Although human GBP1 has been shown to restrict *T. gondii* infection, it does so in a cell type dependent manner. GBP1 restricts infection in IFNγ-treated human mesenchymal stromal cells (MSCs) and lung epithelial cells (i.e. A549 cells) but not myeloid-derived cells (i.e. HAP1 cells)(26-28). GBP1 is also implicated in an inflammasome pathway that results in host cell death in human macrophages following *T. gondii* infection (29). Additionally, GBP5 has been shown to play a role in the clearance of *T. gondii* from human macrophages *in vitro,* albeit in an IFNγ independent manner (30). Humans also possess an ISG15-dependent, IFNγ inducible, noncanonical autophagy (ATG) pathway that restricts *T. gondii* growth in human cervical adenocarcinoma cells (HeLa cells) and A549 cells(31, 32). A similar noncanonical ATG dependent pathway has been reported in human umbilical vein epithelial (HUVEC) cells, although it differs slightly in culminating in lysosome fusion(33). Finally, indoleamine 2,3-dioxygenase (IDO1) has been shown *in vitro* to restrict *T. gondii* growth by limiting L-tryptophan availability in human fibroblasts and monocyte derived macrophages as well as in human derived cell lines of myeloid, foreskin, liver, or cervix origin (e.g. HAP1s, HFFs, Huh7s, and HeLas) but not in cells lines originating from mesenchymal stem cells, the large intestine, or the umbilical endothelium (e.g. MSCs, $CaCO_2$s, or HUVECs)(26, 34-38).

Collectively, the previous studies examining IFNγ mediated growth restriction in human cells support a model where different mechanisms make variable contributions in distinct lineages. However, the known pathways for restriction only cover a small fraction of the genes that are normally upregulated in different human cell types following treatment with IFNγ (7, 39). Hence, there may be additional control mechanisms not yet defined, including either those that are lineage-specific or that operate globally in all cell types. To explore this hypothesis, we screened a library of 414 IFNγ induced interferon stimulated genes (ISGs) in a one gene per well format to attempt to identify novel human factors with the ability to restrict *T. gondii* infection.

Results

To identify novel ISGs that impact *T. gondii* infection, we employed a library of 414 IFNγ induced ISGs cloned into a lentiviral expression cassette co-expressing tagRFP, as previously described by Abrams et al. (10). To screen for ISGs that restrict *T. gondii* infection, we developed a high-throughput method to quantitatively measure infection of GFP-expressing type III strain CTG parasites using automated microscopy. A549 lung epithelial cells were infected with CTG-GFP and the size of individual parasitophorous vacuoles (PVs), the number of vacuoles per field, and the percentage of vacuoles with a size consistent with containing ≥ 8 parasites was determined after 36 hr of culture (**Figure 1A-C**). Cells were transduced with lentivirus in a one gene per well format and challenged with CTG-GFP

(**Figure 1D**). Transduction efficiency was high for most ISGs with 86% (357/414) of ISGs expressed in at least 50% of the cell population and 50% of ISGs (205/414) expressed in 90% of the cell population (**Dataset 1**). Using this approach, we found three ISGs that restricted infection: IRF1, TRIM31, and RARRES3(**Figure 1E, Dataset 1**). All hits were identified as significant by a two-way ANOVA ($P < 0.0001$). We found it curious that IDO1 was not identified by this screen considering its significant impact on infection observed in some but not all cell lines (26, 34-38). There have been no previous reports as to the role of IDO1 during infection in A549s and as such we generated an IDO1 deficient A549 cell line and challenged with CTG-GFP in the presence of IFNγ. Consistent with the results of our screen, IDO1 deficiency did not impair IFNγ-mediated restriction of CTG-GFP suggesting that IDO1 does not play a role in the restriction of *T. gondii* in A549 cells (**Figure 1F**).

Validation of Screen Hits

Cells ectopically expressing IRF1, TRIM31, and RARRES3 expanded normally and showed similar viability compared to a luciferase control when stained with the live-dead stain SYTOX green, suggesting that the overexpression of these genes is not cytotoxic (**Figure 2A-B**). To confirm that these genes restrict *T. gondii* infection, we ectopically expressed these genes in A549 cells and challenged with CTG-GFP for 36 or 96 h. RARRES3 and IRF1 ectopic expression resulted in a reduction in average vacuole size at 36 h (**Figure 2A-B**). At 96 h, the total area infected per well was significantly lower for RARRES3 and IRF1 expressing cells compared to control as was the average size of infection foci (**Figure 2C-D**). TRIM31 had no significant effect on infection in validation experiments and it was not studied further. IRF1 has a known role in amplifying IFNγ mediated transcription, and its role relative to IFNγ is further explored below. RARRES3 is a small, 18.2 kDa single domain protein in the HRASLS family(40). It displays phospholipase A1/2 activity *in vitro* and has been shown to suppress Ras signaling and promote apoptosis(41, 42). Although RARRES3 was described by a previous screen to be antiviral(12), it was not studied further and little is known about its involvement in immunity to other pathogens. In studies described below, we explore its role in restricting growth of intracellular *T .gondii*.

IRF1 versus IFNγ induced genes

In mice, Irf1 deficiency has been shown to result in increased susceptibility to *T. gondii* infection (43), consistent with the secondary induction of a broad set of ISGs downstream of IFN dependent STAT-mediated gene expression(44). However, it is unknown what subset of IFNγ-induced genes are regulated by IRF1 in A549 cells. To define these two gene sets, we ectopically expressed IRF1 or luciferase control in A549 cells, treated a subset of control cells with IFNγ, and analyzed transcriptional changes by RNA-seq. For both IFNγ and IRF1, the majority of changes were due to upregulation and we focused our analysis on these genes (**Figure 3A,B**). We identified 160 genes upregulated by IRF1 and 380 genes upregulated by IFNγ in A549 cells (FDR ≤ 0.05, 2 fold) (**Dataset 2**). When we compared these gene lists with the ISG library with which we challenged *T. gondii* infection, we found that 41.1% (86/160) of IFNγ induced genes and 53.8% (156/380) of IRF1 induced genes were represented by the library (**Dataset 3**). Notably, strongly induced ISGs were more commonly represented in the ISG library with 69% of the top 100 strongest induced genes

by IFNγ and 67% of those induced by IRF1 being represented (**Figure 3C, Dataset 3**). Gene ontology (GO) analysis for the lists of IRF1 and IFNγ induced genes revealed induction of very similar processes that were grouped into IFN signaling, immune response regulation, host defense, and antigen presentation (**Figure 3D-E**). Interestingly, RARRES3 was strongly induced by both IRF1 and IFNγ treatment.

RARRES3 does not affect immune signaling

To determine if the observed reduction in infection with RARRES3 overexpression might also be due to induction of interferon expression and downstream ISG induction, we used CRISPR/Cas9 mediated gene editing to generate a STAT1$^{-/-}$ A549 cell line (**Figure 4A-B**). We ectopically expressed RARRES3 in these cells and subsequently infected with CTG-GFP parasites. The same phenotypes were observed with RARRES3 ectopic expression irrespective of the presence of STAT1, suggesting that decreased infection on over-expression of RARRES3 is not due to induction of IFNγ signaling (**Figure 4C-F**). Interestingly, we noticed that RARRES3 ectopic expression resulted in a modest increase in the number of PVs observed at 36 h in wild type cells and was slightly more pronounced in STAT1$^{-/-}$ cells (**Figure 2C, 4C**). We further tested if ectopic expression of RARRES3 impacted NF-κB or interferon signaling by using κB-, ISRE-, and GAS-luciferase reporter cell lines. RARRES3 did not significantly impact luciferase expression for any of the reporters tested (**Figure 4G-J**). These findings suggest that RARRES3 does not modulate immune signaling pathways and instead plays a direct role in restricting infection.

Endogenous RARRES3 can restrict infection

To determine if endogenously expressed RARRES3 impacts infection, we next used CRISPR/Cas9 mediated gene editing to generate a RARRES3$^{-/-}$ A549 cell line. Alternatively, cells were transduced with an expression cassette containing Cas9 and a previously used nontargeting sgRNA to serve as a negative control(45). RARRES3 deficiency did not alter the susceptibility of quiescent cells to infection (**Figure 5A-B**). However, RARRES3 deficiency partially alleviated IFNγ-mediated restriction of CTG-GFP infection and this deficiency was complemented with RARRES3 ectopic expression (**Figure 5A-B**). As previously mentioned, RNA-seq analysis showed that RARRES3 expression was strongly induced by both IRF1 and IFNγ. Since RARRES3 was the only ISG identified by our screen to restrict *T. gondii* infection, we wanted to determine if the impact of IRF1 on infection was solely due to upregulation of RARRES3 expression. To test this, we ectopically expressed IRF1 or luciferase control in WT and RARRES3$^{-/-}$ A549 cells and challenged them with CTG-GFP. However, loss of RARRES3 did not impact IRF1 mediated restriction of infection (**Figure 5C**). This suggests that either IRF1 mediated infection restriction is RARRES3 independent or involves multiple factors with RARRES3 playing a redundant role in the process of restricting growth. CTG is a type III strain of *T. gondii* that is less virulent in mice and more susceptible to IFNγ mediated restriction than other strains (46-48). We wanted to determine if RARRES3 also impacts other strains of *T. gondii*. To test this, we infected A549s ectopically expressing RARRES3 with GFP expressing RH88 (Type I) and Me49 (Type II). However, RARRES3 had no impact on the infection of

either of these two strains (**Figure S1**). Differential expression or polymorphic virulence factors may explain the disparity in susceptibility to RARRES3 mediated restriction between strains(48, 49).

RARRES3 promotes premature egress

We subsequently revisited our previous finding that infection in RARRES3 ectopically expressing cells results in more, smaller PVs at 36 h than control. This result suggested to us that RARRES3 might be promoting premature egress of the parasite. To test this possibility, we infected A549 cells ectopically expressing RARRES3 with CTG-GFP parasites and measured lactose dehydrogenase (LDH) release (**Figure 6A**). RARRES3 ectopic expression resulted in increased LDH release in CTG-infected cells compared to control cells (**Figure 6A**). We next sought to differentiate if the observed LDH release was due to PKG dependent, active parasite egress or a form of induced cell death. To differentiate between these two hypotheses, we treated cells during infection with a trisubstituted pyrrole *T. gondii* protein kinase G (PKG) inhibitor known as Compound 1(50, 51). Compound 1 is a potent inhibitor of parasite egress and has also been shown to promote differentiation from tachyzoites to bradyzoites, significantly slowing parasite growth thus also delaying or preventing egress(52-54). Treatment with Compound 1 blocked the LDH release observed during infection and compound 1 treated cells did not stain with propidium iodide, suggesting that host cell death as measured by LDH release was due to parasite egress (**Figure 6B, Figure S2A**).

In addition to increased parasite egress, we observed a reduction in host cell number during infection in cells ectopically expressing RARRES3 compared to control (**Figure 6C**). Similar to above, this phenotype was blocked by Compound 1 addition. A common trigger of premature egress is the induction of cell death pathways, of which there is a diversity of types controlled by different mechanisms (55-58). Hence, we were curious if extending this timepoint further would reveal host cell death even with blockage of parasite egress by Compound 1. However, Compound 1 addition during infection resulted in no significant increase in LDH release or propidium iodide staining even 72 h after infection (**Figure 6D, Figure S2B**). Meanwhile, in untreated, infected cultures the cell monolayer was nearly completely lysed and LDH activity was elevated in the supernatant (**Figure 6D, Figure S2C**). Collectively, these findings suggest that induction of cell death by RARRES3 is not the trigger for promotion of parasite egress. To further test this idea, we treated cells with a panel of inhibitors during infection either individually or in combination as indicated (**Figure 6E**). These inhibitors included the pan-caspase inhibitor Z-VAD-FMK, which blocks apoptosis; the necroptosis inhibitors GSK'963, GSK'872, and necrosulfonamide (NSA), which block RIP1, RIP3, and MLKL activity respectively; and the pyroptosis inhibitor Z-YVAD-FMK, which blocks caspase 1. No single drug or combination thereof was capable of inhibiting LDH release during infection except for GSK'872, which partially prevented LDH release in both RARRES3 ectopically expressing and control cells. Overall, we conclude from these experiments that it is unlikely that over expression of RARRES3 induces cell death and therefore it must trigger premature egress by some other means.

A similar premature egress phenotype to that observed here has previously been identified in HFF cells(57). We hypothesized that RARRES3 might play a role in this process. To test this possibility, we ectopically expressed

RARRES3 in HFF cells and infected with CTG-GFP parasites. RARRES3 ectopic expression was found to restrict CTG infection (**Figure 7A-B**). We next ablated RARRES3 expression in HFFs using CRISPR/Cas9 mediated gene editing. Loss of RARRES3 resulted in a partial reduction in IFNγ -dependent cell death in RARRES3$^{-/-}$ HFF cells compared to control cells expressing Cas9 and a nontargeting sgRNA (**Figure 7C**). This finding indicates that RARRES3 plays a role in premature egress but is not the only factor involved in HFF cells. In line with this finding, RARRES3 deficiency in HFF cells partially abrogated IFNγ -mediated restriction of CTG-GFP infection (**Figure 7D**). Moreover, treatment with Compound 1 completely blocked cell death during infection, suggesting that cell death is caused by PKG dependent parasite egress (**Figure 7E, Figure S2D-F**). Collectively, this data suggests that RARRES3 over-expression promotes premature parasite egress independently of host cell death pathways in multiple cell lines which presumably stunts parasite growth leading to reduced infection overall.

Discussion

Although mechanisms of IFNγ-mediated immunity are highly conserved across different cell types in mice, the currently known restriction mechanisms in humans show dramatic differences between cell types with no common or widespread restriction mechanism being observed. However, of the hundreds of ISGs, the vast majority have never been studied in relation to *T. gondii*, leaving open the possibility of unidentified restriction mechanisms. Herein, we performed a screen of IFNγ induced ISGs to identify novel mechanisms of IFNγ-mediated immunity in humans. Our screen identified RARRES3 and IRF1 as ISGs restrictive to *T. gondii* infection in human cells. Further study revealed that RARRES3 induced premature egress of *T. gondii* from host cells in a cell death independent manner. Not unexpectedly, IRF1 induced genes were largely found to be a subset of those induced by IFNγ, including RARRES3. These findings suggest that IRF1 works by the collective action of multiple ISGs. The relative lack of individual ISGs that are active alone also suggest that control mechanisms effective against *T. gondii* rely on complexes of multiple ISGs or cellular proteins working in concert. Hence the control of intracellular eukaryotic pathogens contrasts with that of bacterial and viral pathogens, mirroring differences in their overall biological complexity.

We identified RARRES3 as an ISG promoting premature egress of type III strains of *T. gondii* in two different human cell lines. This phenotype occurs independently of triggering downstream immune signaling. A common cause of premature egress is the induction of host cell death pathways (55-57). And indeed, such a mechanism might be suggested due to the fact that RARRES3 ectopic expression has been previously shown to induce apoptosis(42). However, in our system RARRES3 ectopic expression was not found to impact cell death. Additionally, basal levels of LDH release were not increased in cells ectopically expressing RARRES3. Finally, when we blocked cell death pathways individually or in tandem, we did not see a reduction in LDH. The one exception to this pattern was the reduced release of LDH following treatment with GSK'872. We suspect this result is due to RIP3 inhibition mediated induction of apoptosis as has been demonstrated previously with GSK'872 treatment (59). Thus, following treatment

with GSK'872 it is likely that infection is hindered by host cell apoptosis and LDH release is not observed since cell membranes remain largely intact. The early egress phenotype observed here was similar to an IFNγ dependent premature parasite egress observed in HFF cells that was independent of known cell death pathways(57). We found that ablation of RARRES3 expression partially prevented the IFNγ and infection dependent cell death phenotype in HFF cells. Furthermore, we observed that LDH release was blocked via Compound 1 mediated inhibition of PKG suggesting that RARRES3 over-expression leads to parasite egress resulting in host cell lysis. Although previous studies using CDPK3 inhibition concluded that blocking egress was not sufficient to prevent cell death, our findings differ from this conclusion, possibly due to the stronger role for PKG in controlling egress(53). It is presently unclear how RARRES3 leads to premature egress, although it is possible that its phosphoplipase A1/A2 activity may alter cellular lipid pools that could induce premature egress. As an example of the sensitivity of egress to membrane lipid constituents, increases in phosphatidic acid(60), or the activity of lipolytic lecithin: cholesterol acyltransferase(61) have been shown to trigger egress of *T. gondii*.

In addition to RARRES3, we found that ectopic expression of IRF1 was sufficient to restrict *T. gondii* infection. It was not surprising to us that we identified IRF1 in this screen considering the well-known role of IRF1 in the secondary induction of ISGs and other protective factors downstream of IFN signaling(44). Mice deficient in Irf1 were previously shown to be more susceptible to *T. gondii* infection(43). However, considering the limited number of ISGs found to restrict *T. gondii* infection in our screen, we were curious as to what genes or pathways were being induced by IRF1 ectopic expression and how this compared to IFNγ mediated gene expression in A549s. Although few genes were substantially downregulated by IRF1 expression, 160 genes were upregulated ≥ 2 fold by IRF1 compared to 380 genes with IFNγ treatment. IRF1 induced genes were largely a subset of those IFNγ inducible genes. Notably, this is not always the case with a significant disparity in genes being induced by IRF1 compared to IFNs being reported previously in BEAS-2B cells(62). Overall, similar processes were induced by both IRF1 and IFNγ and these were related to antigen processing and presentation, host defense, and immune signaling. We observed that IRF1 and IFNγ both strongly induced the expression of RARRES3 which led us to question if infection restriction by IRF1 was due to the induction of RARRES3 expression. However, we found that this was not the case, suggesting that RARRES3 either does not play a role in IRF1 mediated restriction of *T. gondii* infection or plays a redundant role. Hence it is likely that IRF1 leads to overexpression of multiple ISGs that collectively inhibit parasite growth.

Although our study is the first to broadly screen ISGs for anti-protozoal activity, it is curious that we only identified two genes that were inhibitory to *T. gondii* infection. In contrast, similar screens challenging viruses and bacteria have commonly identified a minimum of 2-3 times this number of ISGs that were restrictive to infection(10-13). One possible explanation of this difference is that *T. gondii* separates itself from the host cytoplasm via the host derived PVM that forms a barrier to otherwise harmful ISGs in the cytosol. Another explanation is that a common mechanism of ISG activity is the manipulation or shutdown of host processes required for pathogen infection. Examples include PKR and IFIT mediated inhibition of host translation machinery, processes that directly affect viral

infection (7). In contrast, *T. gondii* is a relatively autonomous intracellular pathogen with relatively limited need for host machinery for its growth and replication. Hence, the fact that so few genes were identified by this screen may reflect a secluded existence of T. *gondii* within the PVM and its autonomy of cellular processes relative to viral or bacterial pathogens.

Alternatively, the low number of single genes that restrict growth of *T. gondii* in A549 cells suggests that IFNγ -dependent restriction is a complex process requiring the cooperation of multiple host factors at a time. Hence, the expression of single factors may not be sufficient to restrict infection. For example, a requirement for additional factors could explain why ISG15 was not identified by this screen as ISGylation also requires ubiquitin-like conjugation to attach to target proteins(63). ISG15 knockout was previously found to enhance *T. gondii* growth in A549 cells (31) and this was attributed to its role in the targeting of autophagy machinery to the PV during infection leading to restriction of parasite growth. Currently, over 200 genes have been found to be involved in autophagy in human cells according to the human autophagy database (HADb, http://autophagy.lu/clustering/index.html). Furthermore, coimmunoprecipitation experiments indicated that ISG15 interacts directly or indirectly with more than 240 proteins(31). Thus, although ISG15 may be necessary for autophagy mediated infection restriction as observed with knockout based studies, its individual ectopic expression may not be sufficient to induce this mechanism of infection restriction. A similar explanation can be made for GBP1 that was shown via knockout experiments to be important for restriction of *T. gondii* in A549 cells previously(28). Gbp1 recruitment to the PV and parasite clearance in mice has been shown to require the autophagy machinery(64) and the interaction of GBP1 with ATG5 has been reported in a human cell line(31). In human macrophages, the AIM2 inflammasome has been reported to induce host cell death in a GBP1 dependent manner(29). Thus, the expression of GBP1 individually may not be sufficient to restrict *T. gondii* infection. A similar argument is unlikely to explain the lack of a phenotype for IDO1, which is not thought to require any other genes for its function. However, this pathway does not seem to operate in all human cells(26, 36, 37). Our findings demonstrate that IDO1 does not impact infection specifically in A549s. Finally, it is also possible that ISGs important for *T. gondii* were missed by this screen as the library used herein is not an exhaustive list of all ISGs expressed in A549 cells. Hence it is possible that other ISGs that restrict *T. gondii* infection could be identified using a more focused library or using a similar approach in a different human cell line.

Although we successfully identified a novel anti-parasitic ISG impacting *T. gondii* infection, the scarcity of ISGs identified with the screening approach used here is also of interest. Our results suggest that immunity to *T. gondii* is a complex process requiring multiple factors to impact infection. This complexity differs from other intracellular pathogens such as bacteria and viruses, where single ISGs are often sufficient to inhibit infection. As such, a future loss-of-function based screen for ISGs targeting *T. gondii* infection may reveal additional mechanisms of *T. gondii* restriction.

Acknowledgements

We thank members of the Sibley lab for helpful suggestions. Partially supported by NIH grants (R21 AI154048, R01 AI118426 to L.D.S.). The Welch Foundation (I-1704 to N.M.A.) and the National Institutes of Health (AI083359 to N.M.A.).

Author contributions

Conceptualization: N.R., L.D.S.; Methodology: N.R.; Investigation: N.R.; Formal analysis: N.R.; Resources: M.E.A., S.M.K., J.W.S., N.M.A.; Supervision: L.D.S.; Writing, reviewing, editing: N.R., L.D.S., N.M.A., J.W.S., S.M.K

Conflicts

We state no conflict of interest.

Data deposits

RNASeq data generated here have been deposited to GEO with the accession number GSE181861.

Methods

Cell lines and Parasites

HeLa adenocarcinoma, A549 lung carcinoma (ATCC # CCL-185), HFF foreskin fibroblast (ATCC # SCRC-1041), and human embryonic kidney-derived 293T cells (ATCC # CRL-3216) were grown in DMEM supplemented with 10% FBS, 10 mM HEPES (pH 7.5), 2 mM L-glutamine, and 10 µg/mL gentamicin. Cells were grown at 37° C with 5% CO_2. *Toxoplasma gondii* strains RH88 (Type I), Me49 (Type II), and CTG (Type III) expressing GFP were generated via random insertion of pGRA1.GFP.GRA2.DHFR after electroporation as described previously (65). Clonal populations expressing GFP were generated via limiting dilution. *T. gondii* lines were passaged as described previously in HFFs grown under the conditions listed above(66). Parasite and host cell lines were confirmed to be negative for mycoplasma using an e-Myco plus kit (Intron Biotechnology).

Plasmids and Cloning

The plasmids TRIP.RARRES3 and control constructs were kindly provided by Neal Alto and John Schoggins. Briefly, the TRIP plasmid encodes an expression cassette flanked by lentiviral LTRs. Expression of a bicistronic transcript including tagRFP and a gene of interest is driven by a CMV promoter. The gene of interest and tagRFP are translated independently via an internal ribosome entry site. Cas9 resistant RARRES3 was generated from the WT TRIP.RARRES3 construct by overlap extension PCR. For CRISPR/Cas9 experiments, RARRES3 and nontargeting guides were cloned into plentiCRISPRv2 (Addgene plasmid #52961)(67). Primers for the above cloning are listed in

supplementary table 1. For IDO1, an IDO1 targeting sgRNA was cloned into pLenti-Cas9-GFP (Addgene plasmid #86145). Briefly, pLenti-Cas9-GFP was digested with BsmBI (New England Biolabs). Primers listed in supplemental table 1 were annealed and ligated into the digested plasmid using T4 ligase (New England Biolabs). For the generation of pGRA1.GFP.GRA2.DHFR, an expression cassette consisting of the GRA1 5' UTR (M26007.1, nucleotides 4-615) driving the expression of GFP (MN114103.1, coding sequence) flanked by the GRA2 3' UTR (XM_002366354.2, nucleotides 997-1114) was cloned into pHL931 along with DHFR (XM_002367211.2, coding sequence) expressed from its native promoter and flanked by its 3' UTR (L08489.1).

Lentivirus Production and Cell Line Generation

TRIP lentiviruses were produced as previously described(68). Lentiviruses derived from Lenti-Cas9-GFP, lentiCRISPRv2 and HAGE NFkB-TA-LUC-UBC-GFP-W were produced similarly. Briefly, 293T cells were seeded at 4 x 10^5 cells per well into 6-well plates. Cells were transfected with 1 µg pTRIP, pLenti-Cas9-GFP, plentiCRISPRv2 or pHAGE NFkB-TA-LUC-UBC-GFP-W, 0.2 µg plasmid expressing VSVg, and 0.8 µg plasmid expressing HIV-1 gag-pol using X-tremeGENE 9 (Sigma). Media was changed 6 h later and lentivirus containing culture supernatants were collected at 48 and 72 h post-transfection. Pooled supernatants were clarified by centrifugation at 800 x g for 5 min. Polybrene and HEPES were added to a final concentration of 4 µg/mL and 35 mM respectively. Lentivirus was stored at -80° C until use.

For lentivirus transductions, cells were seeded at 7 x 10^4 cells per well in 24 well plates. The next day, media was changed to DMEM supplemented with 4 µg/mL polybrene, 3% FBS, 35 mM HEPES, 2 mM glutamine, and 10 µg/mL gentamicin. Cells were transduced by spinoculation at 800 x g, 45 min, 37° C. For the ISG screen, media was changed 6 h later to normal growth medium. Cells were replated at 48 h post transduction for subsequent experimentation.

For knockout cell line generation, cells were transduced with lentiCRISPRv2 or pLenti-Cas9-GFP containing the appropriate sgRNA for Cas9 targeting as above. For lentiCRISPRv2, cells were selected for at least two weeks in growth media containing 4 µg/mL puromycin before experimentation. For IDO1$^{-/-}$, STAT1$^{-/-}$ and RARRES3$^{-/-}$ A549 cell lines, cells were transduced with a single lentivirus and clonal cell lineages were established through limiting dilution. For HFFs, a heterogenous bulk population RARRES3 knockout cell line was generated by transducing at a tissue culture infectious dose of 90% ($TCID_{90}$) with two different lentiCRISPRv2 based lentiviruses expressing separate RARRES3 targeting sgRNAs. Nontargeting control cell lines were generated for use as a control in all experiments involving RARRES3$^{-/-}$ cells. Here, cells were transduced with a single lentiCRISPRv2 based lentivirus containing a single nontargeting guide. For RARRES3 and STAT1, editing was confirmed by PCR amplifying targeted loci using primers listed in supplementary table 1 followed by Sanger sequencing. Editing efficiency was quantitated using Synthego ICE analysis (https://ice.synthego.com/#/). For single cell clones, >90% editing was verified. For HFF bulk population knockout of RARRES3, 68% editing of sequenced alleles was observed. For STAT1, editing was further confirmed

functionally via testing the sensitivity of cells to IFN treatment as determined by IRF1 induction. For IDO1, editing was confirmed via loss of protein expression observed by western blot.

Infections

A549 and HeLa cells were seeded at 1.5 x 10^4 in 96 well plates 24 h prior to infection. HFFs were seeded at 2 x 10^4 in 96 well plates 24 h prior to infection. Cells were infected with parasites diluted in 200 µL normal growth medium for 1 h at 37 °C. Media was subsequently changed to 300 µL normal growth medium. For single life cycle infections (typically indicated as 36 h infections), an MOI of 1 was used. For focus forming assay (typically indicated as 96 h infections), an MOI of 0.03 was used. For LDH assays, media was changed to 200 µL normal growth medium. For experiments involving IFNγ, cells were pretreated with or without IFNγ diluted in normal growth medium as indicated for 24 h prior to infection. For infections involving cell death inhibitors or compound 1, drugs were added during the media change after the 1 h infection period. For imaging-based experiments, cells were fixed in 4% formaldehyde for 10 min after infection and washed with PBS before subsequent experimentation.

Drugs

Stocks of the cell death inhibitors Z-VAD-FMK (R&D Systems), GSK'963 (Selleck Chemicals), GSK'872 (Selleck Chemicals), NSA (Tocris), and Z-YVAD-FMK (Sigma) as well as Compound 1 (obtained from MERCK & CO., Inc.) were prepared in DMSO. For use, the drugs were diluted in normal growth medium to the following working concentrations: Z-VAD-FMK (50 µM), GSK'963 (1 µM), GSK'872 (5 µM), NSA (10 µM), Z-YVAD-FMK (10 µM), Compound 1 (5 µM). A DMSO control was included in experiments involving these drugs with a final DMSO concentration of 1%.

LDH Assays

LDH assays were performed with the CyQuant LDH Cytotoxicity Assay Kit (Invitrogen) according to the manufacturer's protocol. Briefly, A549 or HFF cells split in 96-well plates were infected for 1 h as described above with CTG-GFP at an MOI of 40 or 15 respectively and subsequently treated with drugs as indicated. After 36 or 72 h, 20 µL of 10X lysis buffer or PBS was added to each well and incubated at 37° C for 30 min. Afterwards, 50 µL of cell supernatant was mixed with 50 µL of assay buffer and substrate for 30 min at room temperature. The reaction was stopped with 50 µL stop solution and absorbance was measured at 490 nm.

Luciferase Assays

HeLa cells expressing GAS-Fluc, GFP-Fluc, or ISRE-Gluc reporters were transduced with TRIP.RARRES3 or TRIP.Fluc lentivirus as described above. For kB-luc, HeLa cells were additionally transduced with HAGE NFkB-TA-LUC-UBC-GFP-W lentivirus. After 48 h, cells were split into 96 well plates at 1.5 x 10^4 cells/well. Cells were treated with or without 100 U/mL IFNβ or IFNγ as indicated for 24 h and subsequently infected as indicated with CTG-GFP at an MOI of 2 for

24 h**.** For firefly luciferase assays, cells were lysed in 50 µL of 1X Luciferase Cell Culture Lysis Buffer (Promega). For Gaussia luciferase assays, supernatant was collected. Luciferase assays were conducted using Pierce Gaussia Luciferase Glow Assay Kit (Thermo Scientific) or Luciferase Assay System kit (Promega) according to the manufacturer's protocol.

Next Generation RNA-Sequencing Sample Preparation and Analysis

A549 cells transduced with TRIP.IRF1 or TRIP.FLUC derived lentivirus were split at 3.5 x 10^6 into 100 mm dishes. After 24 h, cells were treated with or without IFNγ at 1000 U/mL for an additional 12 h before harvest with RLT buffer. RNA was isolated with a Qiagen RNeasy mini kit according to the manufacturer's protocol. Prior to sequencing, RNA quality was determined on an Agilent Bioanalyzer to have a RIN > 8.0. Libraries prepared from samples were analyzed with an Illumina NovaSeq 6000 S4 generating a minimum of 3 x 10^7 reads per sample. Data was analyzed with Partek Flow software. Prior to alignment, 5 bp were trimmed from the 5' end of transcripts. Only fragments ≥ 25 bp in length were considered for alignment. Alignment was conducted with the STAR aligner and differential expression analysis was conducted using GSA analysis with recommended settings. Genes were characterized here as induced by IFNγ or IRF1 if they induced gene expression ≥ 2 fold with an FDR < 0.05. Gene lists were compared using GeneVenn (http://genevenn.sourceforge.net/index.htm). For GO analysis, gene lists were analyzed with the PANTHER classification system using the GO biological process complete dataset(69, 70). Statistical significance was determined with Fisher's exact test using the Bonferroni correction for multiple testing. Only processes containing at least 25 total genes with a p-value ≤ 0.05 were considered.

Immunofluorescence and Imaging

Samples were fixed in 4% formaldehyde for 10 min at room temperature. Wash buffer (WB) consisted of 1% FBS, 1% normal goat serum (NGS), and 0.02% Saponin in PBS. Samples were blocked for 30 min with PBS containing 5% FBS, 5% NGS, and 0.02% Saponin. Samples were incubated with 1:2000 anti-RFP antibody (Invitrogen) and 1:2000 anti-GFP (Invitrogen) in WB overnight, washed 4 times in WB for 5 min each, and probed with 1:1000 goat anti-mouse Alexa Fluor 488 (Life Technologies) and 1:1000 goat anti-rabbit Alexa Fluor 568 (Life Technologies) in WB for 1 h. For IRF1 staining, 1:500 anti-IRF1 primary antibody (Cell Signaling Technology) and 1:1000 anti-rabbit Alexa Fluor 488 secondary antibody (Life Technologies) were used instead. Samples were washed 3 times with WB and nuclei were stained for 5 min with Hoechst 33342 (Life Technologies) in WB. Samples were imaged with a Cytation 3 imager (BioTek) and images were analyzed in CellProfiler v3.1.9.

Western Blotting

A549 cells were split at 2.5x10^5 cells per well into 6-well plates in standard growth medium. The following day, media was changed to standard growth medium supplemented with or without 1000 U/mL IFNγ. After 24 h, cells were washed with PBS, trypsinized with 0.05% trypsin, and spun down at 200 x g for 5 min. Cell pellets were

washed once with PBS and lysed with CelLytic M (Millipore) supplemented with 20 mM DTT and 125 U/mL benzonase (Millipore). Samples were incubated at room temperature for 20 min, run on a 10%, 37.5:1 polyacrylamide gel, and transferred to nitrocellulose membranes. Membranes were blocked with 0.1% Tween-20 PBS-T containing 5% bovine serum albumin (BSA) for 30 min. Membranes were incubated with 1:1000 rabbit anti-IDO1 (Cell Signaling) and 1:5000 mouse anti-actin (Sigma) in 5% BSA PBS-T for 1 h, washed 4 times with PBS-T for 3 min each, incubated with 1:5000 goat anti-mouse 680RD (LI-COR) and 1:5000 goat anti-rabbit 800CW (LI-COR) in 5% BSA PBS-T for 30 min, washed 4 times in PBS-T for 3 min each, and washed 2 times in PBS. Membranes were imaged with a LI-COR Odyssey scanner.

Statistical Analysis

For most datasets including those normalized to control, statistical significance was determined with a two-way ANOVA and Tukey's honestly significant difference post-hoc test conducted on raw data prior to normalization and considered variance between experimental replicates and variance between experimental conditions. For LDH and luciferase reporter experiments, statistical significance was determined after normalization and considered variance between experimental replicates and variance between experimental conditions. For experiments in Figure 2A and 2B, statistical significance was determined using a Brown-Forsythe and Welch ANOVA. Specifically for datasets not normalized to control with only two conditions, a Mann-Whitney U test was used to determined statistical significance. The term 'technical replicate' refers to separate samples derived from the same original source within the same experiment (i.e. wells of a plate) processed on the same day. The term 'biological replicate' refers to separate experiments conducted on different dates with different samples.

References

1. Furtado JM, Smith JR, Belfort R, Jr., Gattey D, Winthrop KL. 2011. Toxoplasmosis: a global threat. Journal of global infectious diseases 3:281-284.
2. Weiss LM, Dubey JP. 2009. Toxoplasmosis: A history of clinical observations. International journal for parasitology 39:895-901.
3. Furtado JM, Winthrop KL, Butler NJ, Smith JR. 2013. Ocular toxoplasmosis I: parasitology, epidemiology and public health. Clinical & Experimental Ophthalmology 41:82-94.
4. Fisch D, Clough B, Frickel E-M. 2019. Human immunity to Toxoplasma gondii. PLoS pathogens 15:e1008097-e1008097.
5. Alspach E, Lussier DM, Schreiber RD. 2019. Interferon γ and Its Important Roles in Promoting and Inhibiting Spontaneous and Therapeutic Cancer Immunity. Cold Spring Harbor perspectives in biology 11:a028480.
6. Lazear HM, Schoggins JW, Diamond MS. 2019. Shared and Distinct Functions of Type I and Type III Interferons. Immunity 50:907-923.
7. Schoggins JW. 2019. Interferon-Stimulated Genes: What Do They All Do? Annual Review of Virology 6:567-584.

8. van Boxel-Dezaire AHH, Stark GR. 2007. Cell Type-Specific Signaling in Response to Interferon-γ, p 119-154. *In* Pitha PM (ed), Interferon: The 50th Anniversary doi:10.1007/978-3-540-71329-6_7. Springer Berlin Heidelberg, Berlin, Heidelberg.
9. van Boxel-Dezaire AHH, Rani MRS, Stark GR. 2006. Complex Modulation of Cell Type-Specific Signaling in Response to Type I Interferons. Immunity 25:361-372.
10. Abrams ME, Johnson KA, Perelman SS, Zhang L-s, Endapally S, Mar KB, Thompson BM, McDonald JG, Schoggins JW, Radhakrishnan A, Alto NM. 2020. Oxysterols provide innate immunity to bacterial infection by mobilizing cell surface accessible cholesterol. Nature Microbiology 5:929-942.
11. Schoggins JW, Wilson SJ, Panis M, Murphy MY, Jones CT, Bieniasz P, Rice CM. 2011. A diverse range of gene products are effectors of the type I interferon antiviral response. Nature 472:481-5.
12. Schoggins JW, MacDuff DA, Imanaka N, Gainey MD, Shrestha B, Eitson JL, Mar KB, Richardson RB, Ratushny AV, Litvak V, Dabelic R, Manicassamy B, Aitchison JD, Aderem A, Elliott RM, García-Sastre A, Racaniello V, Snijder EJ, Yokoyama WM, Diamond MS, Virgin HW, Rice CM. 2014. Pan-viral specificity of IFN-induced genes reveals new roles for cGAS in innate immunity. Nature 505:691-5.
13. Perelman SS, Abrams ME, Eitson JL, Chen D, Jimenez A, Mettlen M, Schoggins JW, Alto NM. 2016. Cell-Based Screen Identifies Human Interferon-Stimulated Regulators of Listeria monocytogenes Infection. PLoS Pathog 12:e1006102.
14. Suzuki Y, Orellana MA, Schreiber RD, Remington JS. 1988. Interferon-gamma: the major mediator of resistance against Toxoplasma gondii. Science 240:516-8.
15. McCabe RE, Luft BJ, Remington JS. 1984. Effect of murine interferon gamma on murine toxoplasmosis. J Infect Dis 150:961-2.
16. Shirahata T, Shimizu K. 1980. Production and properties of immune interferon from spleen cell cultures of Toxoplasma-infected mice. Microbiology and immunology 24:1109-1120.
17. Gazzinelli RT, Mendonça-Neto R, Lilue J, Howard J, Sher A. 2014. Innate resistance against Toxoplasma gondii: an evolutionary tale of mice, cats, and men. Cell host & microbe 15:132-138.
18. MacMicking JD. 2012. Interferon-inducible effector mechanisms in cell-autonomous immunity. Nat Rev Immunol 12:367-82.
19. Hunter CA, Sibley LD. 2012. Modulation of innate immunity by Toxoplasma gondii virulence effectors. Nature reviews Microbiology 10:766-778.
20. Khan IA, Schwartzman JD, Matsuura T, Kasper LH. 1997. A dichotomous role for nitric oxide during acute Toxoplasma gondii infection in mice. Proc Natl Acad Sci U S A 94:13955-60.
21. Adams LB, Hibbs JB, Taintor RR, Krahenbuhl JL. 1990. Microbiostatic effect of murine-activated macrophages for Toxoplasma gondii. Role for synthesis of inorganic nitrogen oxides from L-arginine. The Journal of Immunology 144:2725.
22. Meisel R, Brockers S, Heseler K, Degistirici Ö, Bülle H, Woite C, Stuhlsatz S, Schwippert W, Jäger M, Sorg R, Henschler R, Seissler J, Dilloo D, Däubener W. 2011. Human but not murine multipotent mesenchymal stromal cells exhibit broad-spectrum antimicrobial effector function mediated by indoleamine 2,3-dioxygenase. Leukemia 25:648-654.
23. Pfefferkorn ER, Eckel M, Rebhun S. 1986. Interferon-gamma suppresses the growth of Toxoplasma gondii in human fibroblasts through starvation for tryptophan. Mol Biochem Parasitol 20:215-24.
24. Meira CS, Pereira-Chioccola VL, Vidal JE, de Mattos CCB, Motoie G, Costa-Silva TA, Gava R, Frederico FB, de Mattos LC, Toxoplasma G. 2014. Cerebral and ocular toxoplasmosis related with IFN-γ, TNF-α, and IL-10 levels. Frontiers in microbiology 5:492-492.
25. Bekpen C, Hunn JP, Rohde C, Parvanova I, Guethlein L, Dunn DM, Glowalla E, Leptin M, Howard JC. 2005. The interferon-inducible p47 (IRG) GTPases in vertebrates: loss of the cell autonomous resistance mechanism in the human lineage. Genome biology 6:R92-R92.
26. Qin A, Lai D-H, Liu Q, Huang W, Wu Y-P, Chen X, Yan S, Xia H, Hide G, Lun Z-R, Ayala FJ, Xiang AP. 2017. Guanylate-binding protein 1 (GBP1) contributes to the immunity of human mesenchymal stromal cells against Toxoplasma gondii. Proceedings of the National Academy of Sciences of the United States of America 114:1365-1370.

27. Ohshima J, Lee Y, Sasai M, Saitoh T, Su Ma J, Kamiyama N, Matsuura Y, Pann-Ghill S, Hayashi M, Ebisu S, Takeda K, Akira S, Yamamoto M. 2014. Role of mouse and human autophagy proteins in IFN-gamma-induced cell-autonomous responses against Toxoplasma gondii. J Immunol 192:3328-35.
28. Johnston AC, Piro A, Clough B, Siew M, Virreira Winter S, Coers J, Frickel E-M. 2016. Human GBP1 does not localize to pathogen vacuoles but restricts Toxoplasma gondii. Cellular microbiology 18:1056-1064.
29. Fisch D, Bando H, Clough B, Hornung V, Yamamoto M, Shenoy AR, Frickel EM. 2019. Human GBP1 is a microbe-specific gatekeeper of macrophage apoptosis and pyroptosis. Embo j doi:10.15252/embj.2018100926.
30. Matta SK, Patten K, Wang Q, Kim BH, MacMicking JD, Sibley LD. 2018. NADPH Oxidase and Guanylate Binding Protein 5 Restrict Survival of Avirulent Type III Strains of Toxoplasma gondii in Naive Macrophages. mBio 9.
31. Bhushan J, Radke JB, Perng YC, McAllaster M, Lenschow DJ, Virgin HW, Sibley LD. 2020. ISG15 Connects Autophagy and IFN-γ-Dependent Control of Toxoplasma gondii Infection in Human Cells. mBio 11.
32. Selleck EM, Orchard RC, Lassen KG, Beatty WL, Xavier RJ, Levine B, Virgin HW, Sibley LD. 2015. A Noncanonical Autophagy Pathway Restricts Toxoplasma gondii Growth in a Strain-Specific Manner in IFN-gamma-Activated Human Cells. MBio 6:e01157-15.
33. Clough B, Wright JD, Pereira PM, Hirst EM, Johnston AC, Henriques R, Frickel EM. 2016. K63-Linked Ubiquitination Targets Toxoplasma gondii for Endo-lysosomal Destruction in IFNγ-Stimulated Human Cells. PLoS Pathog 12:e1006027.
34. Bando H, Sakaguchi N, Lee Y, Pradipta A, Ma JS, Tanaka S, Lai D-H, Liu J, Lun Z-R, Nishikawa Y, Sasai M, Yamamoto M. 2018. Toxoplasma Effector TgIST Targets Host IDO1 to Antagonize the IFN-γ-Induced Anti-parasitic Response in Human Cells. Frontiers in immunology 9:2073-2073.
35. Pfefferkorn ER. 1984. Interferon gamma blocks the growth of Toxoplasma gondii in human fibroblasts by inducing the host cells to degrade tryptophan. Proc Natl Acad Sci U S A 81:908-12.
36. Woodman JP, Dimier IH, Bout DT. 1991. Human endothelial cells are activated by IFN-gamma to inhibit Toxoplasma gondii replication. Inhibition is due to a different mechanism from that existing in mouse macrophages and human fibroblasts. The Journal of Immunology 147:2019.
37. Dimier IH, Bout DT. 1997. Inhibition of Toxoplasma gondii replication in IFN-gamma-activated human intestinal epithelial cells. Immunol Cell Biol 75:511-4.
38. Schmitz JL, Carlin JM, Borden EC, Byrne GI. 1989. Beta interferon inhibits Toxoplasma gondii growth in human monocyte-derived macrophages. Infect Immun 57:3254-6.
39. Rusinova I, Forster S, Yu S, Kannan A, Masse M, Cumming H, Chapman R, Hertzog PJ. 2013. INTERFEROME v2.0: an updated database of annotated interferon-regulated genes. Nucleic Acids Research 41:D1040-D1046.
40. Mardian EB, Bradley RM, Duncan RE. 2015. The HRASLS (PLA/AT) subfamily of enzymes. J Biomed Sci 22:99.
41. Uyama T, Jin X-H, Tsuboi K, Tonai T, Ueda N. 2009. Characterization of the human tumor suppressors TIG3 and HRASLS2 as phospholipid-metabolizing enzymes. Biochimica et Biophysica Acta (BBA) - Molecular and Cell Biology of Lipids 1791:1114-1124.
42. Tsai F-M, Shyu R-Y, Jiang S-Y. 2007. RIG1 suppresses Ras activation and induces cellular apoptosis at the Golgi apparatus. Cellular Signalling 19:989-999.
43. Khan IA, Matsuura T, Fonseka S, Kasper LH. 1996. Production of nitric oxide (NO) is not essential for protection against acute Toxoplasma gondii infection in IRF-1-/- mice. The Journal of Immunology 156:636.
44. Feng H, Zhang Y-B, Gui J-F, Lemon SM, Yamane D. 2021. Interferon regulatory factor 1 (IRF1) and anti-pathogen innate immune responses. PLOS Pathogens 17:e1009220.
45. Doench JG, Fusi N, Sullender M, Hegde M, Vaimberg EW, Donovan KF, Smith I, Tothova Z, Wilen C, Orchard R, Virgin HW, Listgarten J, Root DE. 2016. Optimized sgRNA design to maximize activity and minimize off-target effects of CRISPR-Cas9. Nat Biotechnol 34:184-191.
46. Khaminets A, Hunn JP, Könen-Waisman S, Zhao YO, Preukschat D, Coers J, Boyle JP, Ong YC, Boothroyd JC, Reichmann G, Howard JC. 2010. Coordinated loading of IRG resistance GTPases on to the Toxoplasma gondii parasitophorous vacuole. Cell Microbiol 12:939-61.
47. Boothroyd JC, Grigg ME. 2002. Population biology of Toxoplasma gondii and its relevance to human infection: do different strains cause different disease? Current Opinion in Microbiology 5:438-442.

48. Saeij JPJ, Boyle JP, Coller S, Taylor S, Sibley LD, Brooke-Powell ET, Ajioka JW, Boothroyd JC. 2006. Polymorphic secreted kinases are key virulence factors in toxoplasmosis. Science (New York, NY) 314:1780-1783.
49. Rosowski EE, Lu D, Julien L, Rodda L, Gaiser RA, Jensen KDC, Saeij JPJ. 2011. Strain-specific activation of the NF-kappaB pathway by GRA15, a novel Toxoplasma gondii dense granule protein. The Journal of experimental medicine 208:195-212.
50. Gurnett AM, Liberator PA, Dulski PM, Salowe SP, Donald RG, Anderson JW, Wiltsie J, Diaz CA, Harris G, Chang B, Darkin-Rattray SJ, Nare B, Crumley T, Blum PS, Misura AS, Tamas T, Sardana MK, Yuan J, Biftu T, Schmatz DM. 2002. Purification and molecular characterization of cGMP-dependent protein kinase from Apicomplexan parasites. A novel chemotherapeutic target. J Biol Chem 277:15913-22.
51. Donald RGK, Zhong T, Wiersma H, Nare B, Yao D, Lee A, Allocco J, Liberator PA. 2006. Anticoccidial kinase inhibitors: Identification of protein kinase targets secondary to cGMP-dependent protein kinase. Molecular and Biochemical Parasitology 149:86-98.
52. Nare B, Allocco JJ, Liberator PA, Donald RG. 2002. Evaluation of a cyclic GMP-dependent protein kinase inhibitor in treatment of murine toxoplasmosis: gamma interferon is required for efficacy. Antimicrob Agents Chemother 46:300-7.
53. Lourido S, Tang K, Sibley LD. 2012. Distinct signalling pathways control Toxoplasma egress and host-cell invasion. The EMBO journal 31:4524-4534.
54. Radke JR, Donald RG, Eibs A, Jerome ME, Behnke MS, Liberator P, White MW. 2006. Changes in the expression of human cell division autoantigen-1 influence Toxoplasma gondii growth and development. PLoS pathogens 2:e105-e105.
55. Yao Y, Liu M, Ren C, Shen J, Ji Y. 2017. Exogenous tumor necrosis factor-alpha could induce egress of Toxoplasma gondii from human foreskin fibroblast cells. Parasite (Paris, France) 24:45-45.
56. Persson EK, Agnarson AM, Lambert H, Hitziger N, Yagita H, Chambers BJ, Barragan A, Grandien A. 2007. Death Receptor Ligation or Exposure to Perforin Trigger Rapid Egress of the Intracellular Parasite *Toxoplasma gondii*. The Journal of Immunology 179:8357.
57. Niedelman W, Sprokholt JK, Clough B, Frickel E-M, Saeij JPJ. 2013. Cell death of gamma interferon-stimulated human fibroblasts upon Toxoplasma gondii infection induces early parasite egress and limits parasite replication. Infection and immunity 81:4341-4349.
58. Rosenberg A, Sibley LD. 2021. Toxoplasma gondii secreted effectors co-opt host repressor complexes to inhibit necroptosis. Cell Host Microbe 29:1186-1198.e8.
59. Tenev T, Bianchi K, Darding M, Broemer M, Langlais C, Wallberg F, Zachariou A, Lopez J, MacFarlane M, Cain K, Meier P. 2011. The Ripoptosome, a Signaling Platform that Assembles in Response to Genotoxic Stress and Loss of IAPs. Molecular Cell 43:432-448.
60. Bisio H, Lunghi M, Brochet M, Soldati-Favre D. 2019. Phosphatidic acid governs natural egress in Toxoplasma gondii via a guanylate cyclase receptor platform. Nature Microbiology 4:420-428.
61. Pszenny V, Ehrenman K, Romano JD, Kennard A, Schultz A, Roos DS, Grigg ME, Carruthers VB, Coppens I. 2016. A Lipolytic Lecithin:Cholesterol Acyltransferase Secreted by Toxoplasma Facilitates Parasite Replication and Egress. J Biol Chem 291:3725-46.
62. Panda D, Gjinaj E, Bachu M, Squire E, Novatt H, Ozato K, Rabin RL. 2019. IRF1 Maintains Optimal Constitutive Expression of Antiviral Genes and Regulates the Early Antiviral Response. 10.
63. Perng Y-C, Lenschow DJ. 2018. ISG15 in antiviral immunity and beyond. Nature Reviews Microbiology 16:423-439.
64. Selleck EM, Fentress SJ, Beatty WL, Degrandi D, Pfeffer K, Virgin HWt, Macmicking JD, Sibley LD. 2013. Guanylate-binding protein 1 (Gbp1) contributes to cell-autonomous immunity against Toxoplasma gondii. PLoS pathogens 9:e1003320-e1003320.
65. Shen B, Brown K, Long S, Sibley LD. 2017. Development of CRISPR/Cas9 for Efficient Genome Editing in Toxoplasma gondii, p 79-103. *In* Reeves A (ed), In Vitro Mutagenesis: Methods and Protocols doi:10.1007/978-1-4939-6472-7_6. Springer New York, New York, NY.
66. Khan A, Grigg ME. 2017. Toxoplasma gondii: Laboratory Maintenance and Growth. Current protocols in microbiology 44:20C.1.1-20C.1.17.
67. Sanjana NE, Shalem O, Zhang F. 2014. Improved vectors and genome-wide libraries for CRISPR screening. Nat Methods 11:783-4.

68. Schoggins JW, Dorner M, Feulner M, Imanaka N, Murphy MY, Ploss A, Rice CM. 2012. Dengue reporter viruses reveal viral dynamics in interferon receptor-deficient mice and sensitivity to interferon effectors in vitro. Proc Natl Acad Sci U S A 109:14610-5.
69. Thomas PD, Campbell MJ, Kejariwal A, Mi H, Karlak B, Daverman R, Diemer K, Muruganujan A, Narechania A. 2003. PANTHER: a library of protein families and subfamilies indexed by function. Genome research 13:2129-2141.
70. Thomas PD, Kejariwal A, Guo N, Mi H, Campbell MJ, Muruganujan A, Lazareva-Ulitsky B. 2006. Applications for protein sequence–function evolution data: mRNA/protein expression analysis and coding SNP scoring tools. Nucleic Acids Research 34:W645-W650.

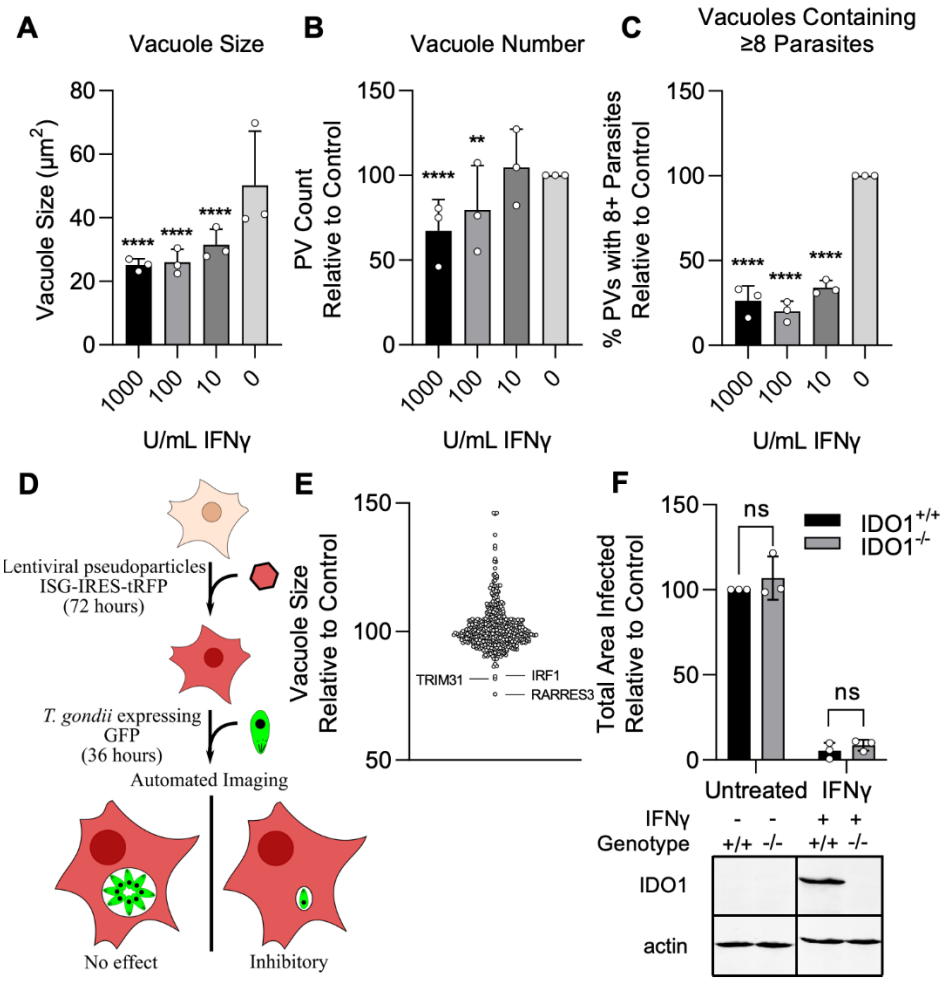

Figure Legends

Figure 1. Screen for interferon stimulated genes (ISGs) impacting *T. gondii* infection. A549 cells were treated with indicated concentrations of IFNγ for 24 h and subsequently infected with the type III strain CTG expressing GFP (CTG-GFP) for 36 h (A-C). Cells were fixed, stained with anti-GFP and anti-RFP antibodies, and imaged using a Cytation3 Imager. (A-C) Average parasitophorous vacuole (PV) size (A), PVs per field (B), and the percentage of vacuoles containing ≥8 parasites (C) was quantitated for data from 36 h image sets. (D) Illustration of the method used to conduct the screen presented in E. (E) A549 cells were transduced with a lentiviral expression cassette co-transcriptionally expressing tagRFP and an ISG of interest in a one gene per well format. After 72 h cells were infected with CTG-GFP for 36 h, fixed, stained with anti-GFP and anti-RFP antibodies, and imaged with a Cytation3 Imager. (F) WT and IDO1$^{-/-}$ A549 cells were infected with CTG-GFP for 96 h. Cells were fixed, stained with anti-SAG1 antibody, and imaged with a Cytation3 Imager. Average total infected area per well is shown. Loss of IDO1 in IDO1$^{-/-}$ A549 cells was confirmed via western blot. Briefly, cells were treated with or without 1000 U/mL IFNγ for 24 h before samples were harvested and IDO1 expression was determined. (A-C, F) Data represent the mean ± standard deviation of three biological replicates conducted in technical triplicate. (E) Data represent mean ± standard deviation of two biological

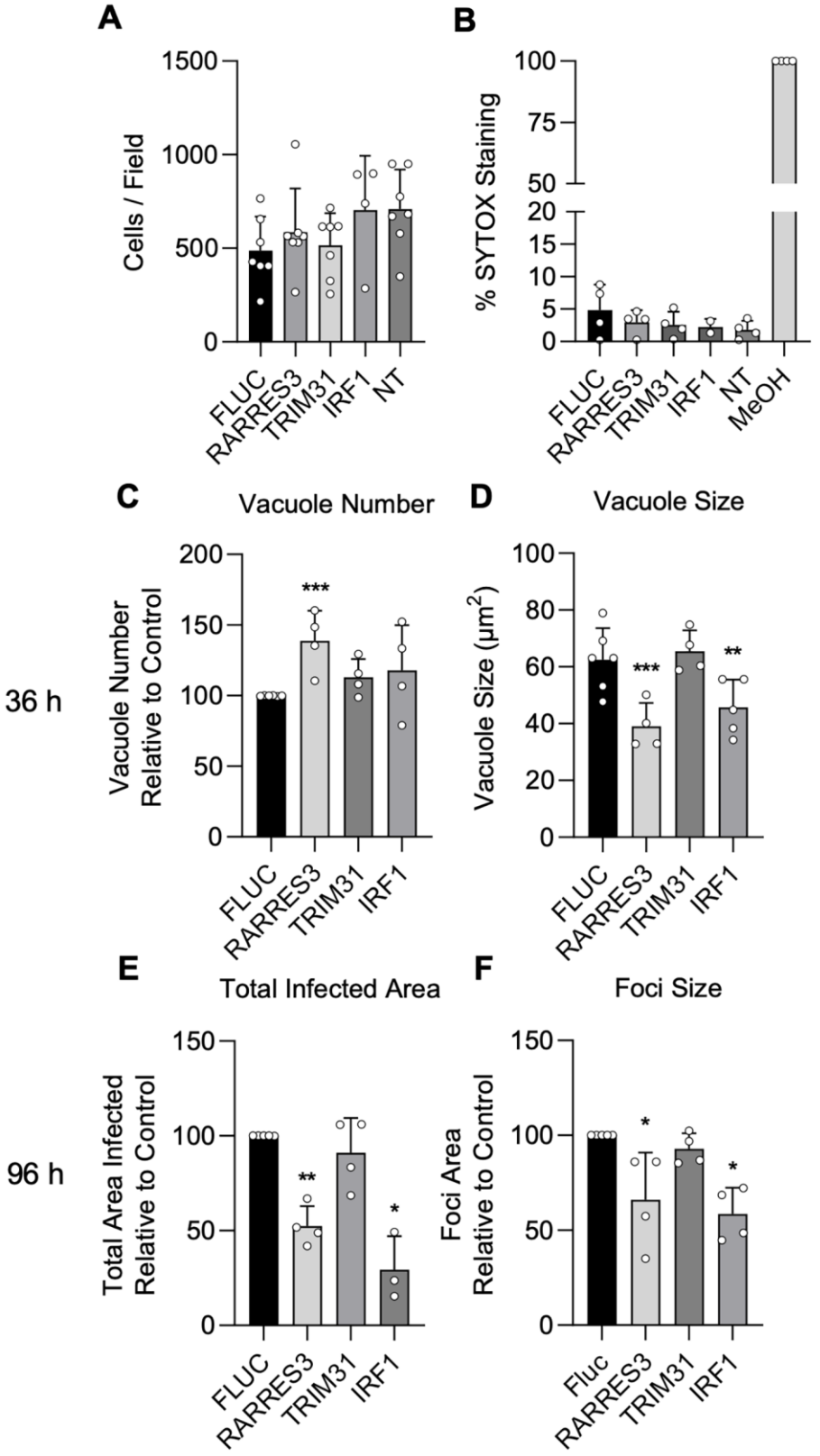

replicates conducted in technical duplicate. Statistical significance was determined using two-way ANOVA with Tukey's test for post-hoc analysis. ns (not significant) $P > 0.05$, ** $P < 0.01$, **** $P < 0.0001$.

Figure 2. IRF1 and RARRES3 restrict *Toxoplasma* infection. (A-B) Wild type (WT) A549 cells were either not transduced (NT) or transduced with TRIP.RARRES3 or TRIP.FLUC control and split 48 h later. After 60 h, cells were stained with Hoechst 33342, SYTOX green, and imaged with a Cytation3 imager. As a positive control, cells were permeabilized by treatment with methanol (MeOH) for 5 min prior to staining. Average cell number (A) and the percentage of SYTOX staining cells (B) were determined. (C-F) WT A549 cells were transduced with TRIP.RARRES3 or TRIP.FLUC control and infected 72 h later with CTG-GFP for 36 (C-D) or 96 (E-F) h. Cells were fixed, stained with anti-GFP and anti-RFP antibodies, and imaged using a Cytation3 Imager. Average PV number per field (C) and PV size (D) were quantitated for 36 h infections while total area infected per sample (E) and average foci size (F) were quantitated for 96 h infections. Data in A represent four to seven biological replicates conducted in technical triplicate. Data in B represent two to four biological replicates conducted in technical triplicate. Data in C-F represent three to four biological replicates

conducted in technical triplicate. Statistical significance was determined using a Brown-Forsythe and Welch ANOVA (A-B) or a two-way ANOVA with Tukey's test for post-hoc analysis (C-F). * $P \leq 0.05$, ** $P < 0.01$.

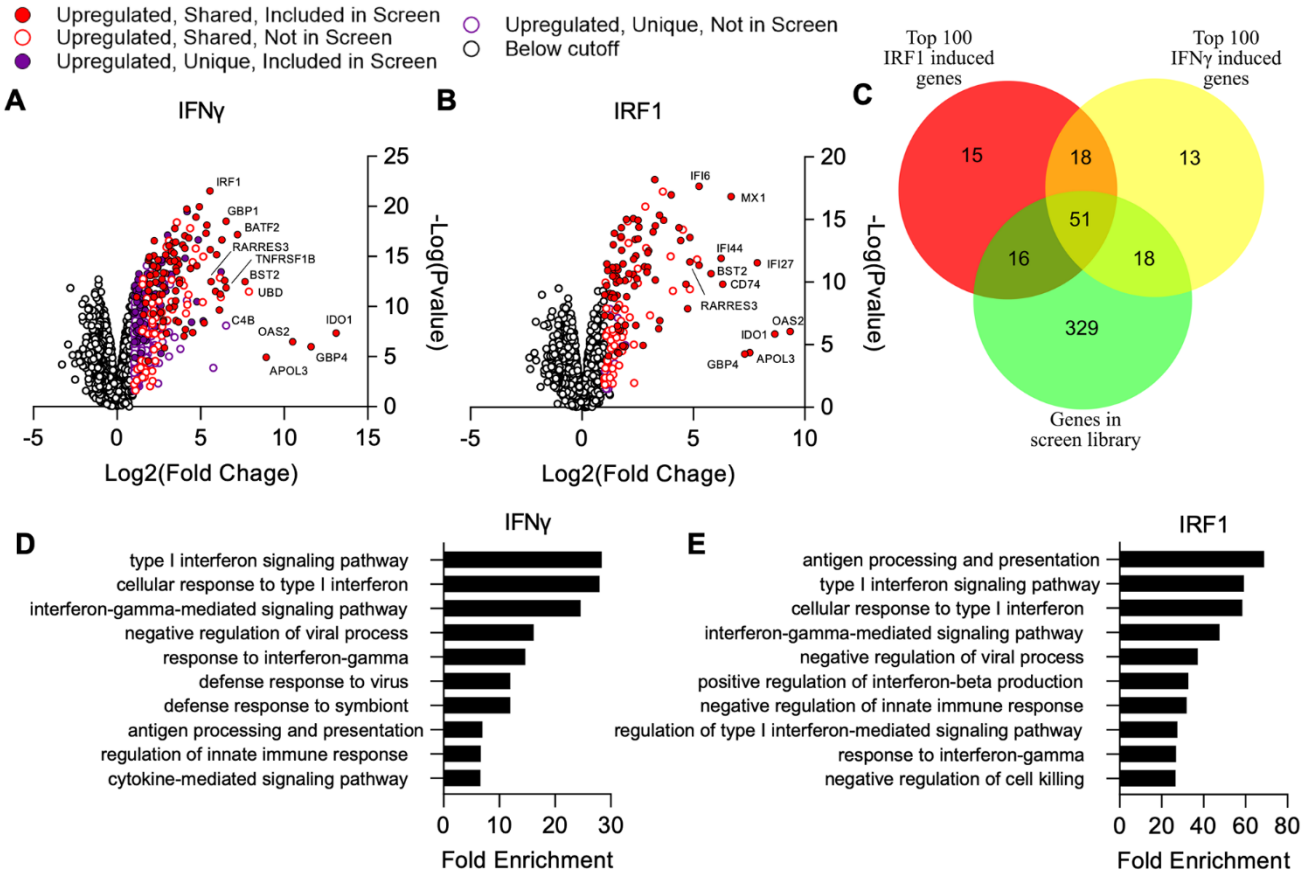

Figure 3. Comparison of genes induced by IRF1 and IFNγ in A549 cells. Cells were transduced with TRIP.IRF1 or TRIP.FLUC control lentivirus. Cells transduced with FLUC were further treated 72 h later with or without 1000 U/mL IFNγ for 24 h. All cell populations were subsequently harvested and analyzed by RNA-Seq. (A-B) Changes in gene expression relative to FLUC control expressing cells for cells treated with IFNγ (A) or ectopically expressing IRF1 (B). (C) Comparison of genes induced ≥ 2 fold with a false discovery rate cutoff of 0.05 by each condition and their overlap with the ISG library used in the screen described in figure 1. (D-E) Lists of induced genes were analyzed with PANTHER gene ontology analysis. The top ten most enriched processes amongst genes induced by IFNγ (D) and IRF1 (E) are shown. Redundant terms were excluded from these lists with only the most enriched version of each term remaining.

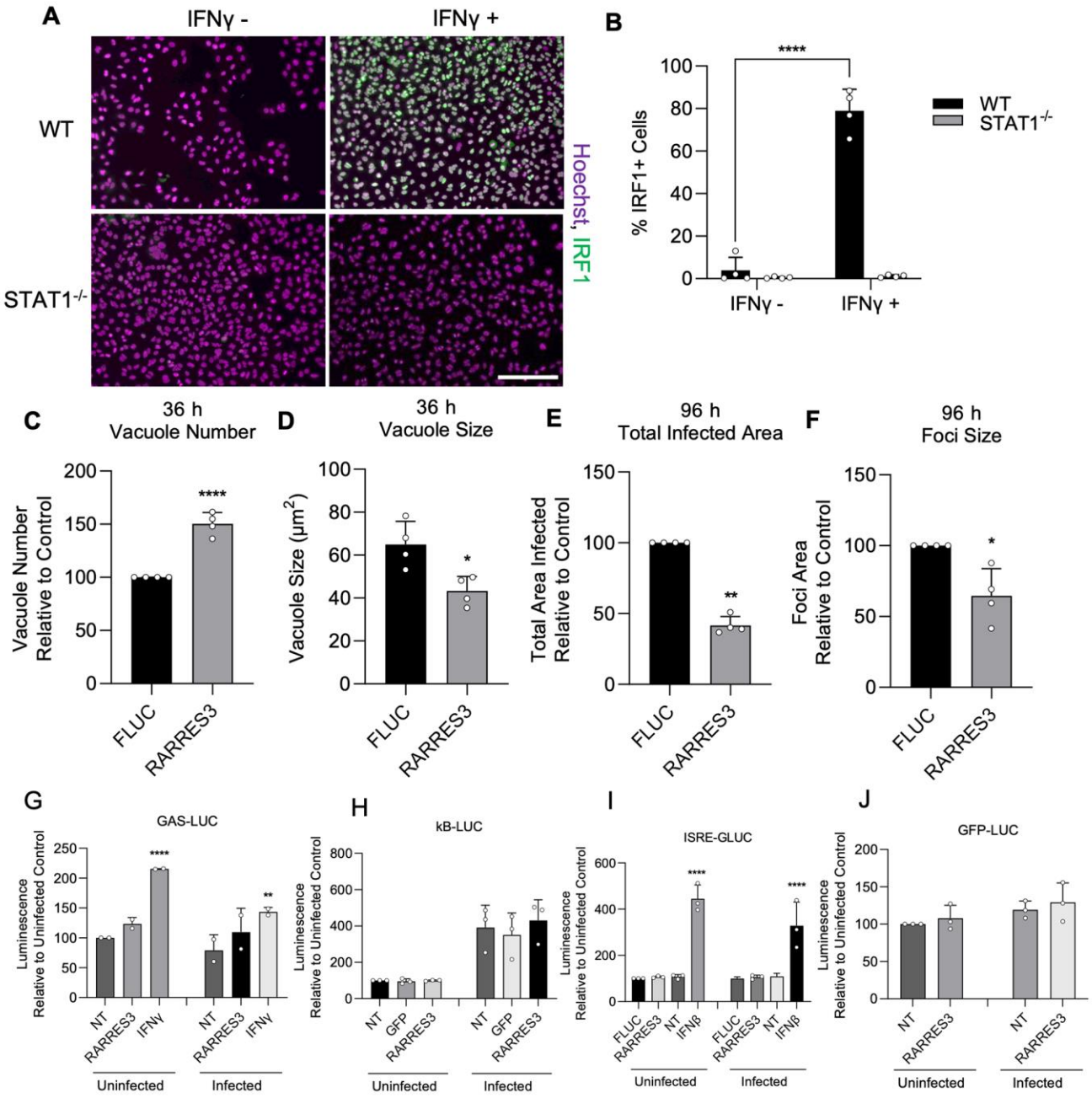

Figure 4. RARRES3 restricts *Toxoplasma* infection in a STAT1 independent manner.

To determine if restriction of *T. gondii* growth was STAT1 dependent, STAT1$^{-/-}$ A549 cells were generated. To confirm complete insensitivity to interferon treatment, WT or STAT1$^{-/-}$ A549 cells were treated with or without 4,000 U/mL IFNγ for 6 h, fixed, stained with anti-IRF1 antibodies, and imaged with a Cytation3 Imager. (A) Representative images and (B) quantitation are shown. Scale bar = 50 μm. (C-F) STAT1$^{-/-}$ A549 cells were transduced with TRIP.RARRES3 or TRIP.FLUC control and infected 72 h later with CTG-GFP for 36 (C-D) or 96 (E-F) h. Cells were fixed, stained with anti-GFP and anti-RFP antibodies, and imaged using a Cytation3 Imager. Average PV number per field (C) and PV size (D) were quantitated for 36 h infections while total area infected per sample (E) and average foci size (F) were quantitated for 96 h infections. HeLa reporter cell lines expressing GAS-LUC (G), kB-LUC (H), ISRE-GLUC (I), and GFP-

LUC (J) were either not transduced (NT) or transduced with TRIP.RARRES3, TRIP.FLUC, or TRIP.GFP. After 72 h, cells were mock treated or treated with 100 U/mL IFNβ or IFNγ as indicated and infected with CTG-GFP for 36 h. Cells were harvested for luciferase assay. Data in B represent means ± S.D. of four biological replicates conducted in technical duplicate. Data in C-F represent means ± standard deviation of four biological replicates conducted in technical triplicate. Data represent means ± S.D. of two (G) or three (H-I) biological replicates conducted in technical duplicate. Statistical significance was determined using two-way ANOVA with Tukey's test for post-hoc analysis except for D where Mann-Whitney's U test was used. * $P \leq 0.05$, ** $P < 0.01$, *** $P < 0.001$, **** $P < 0.0001$.

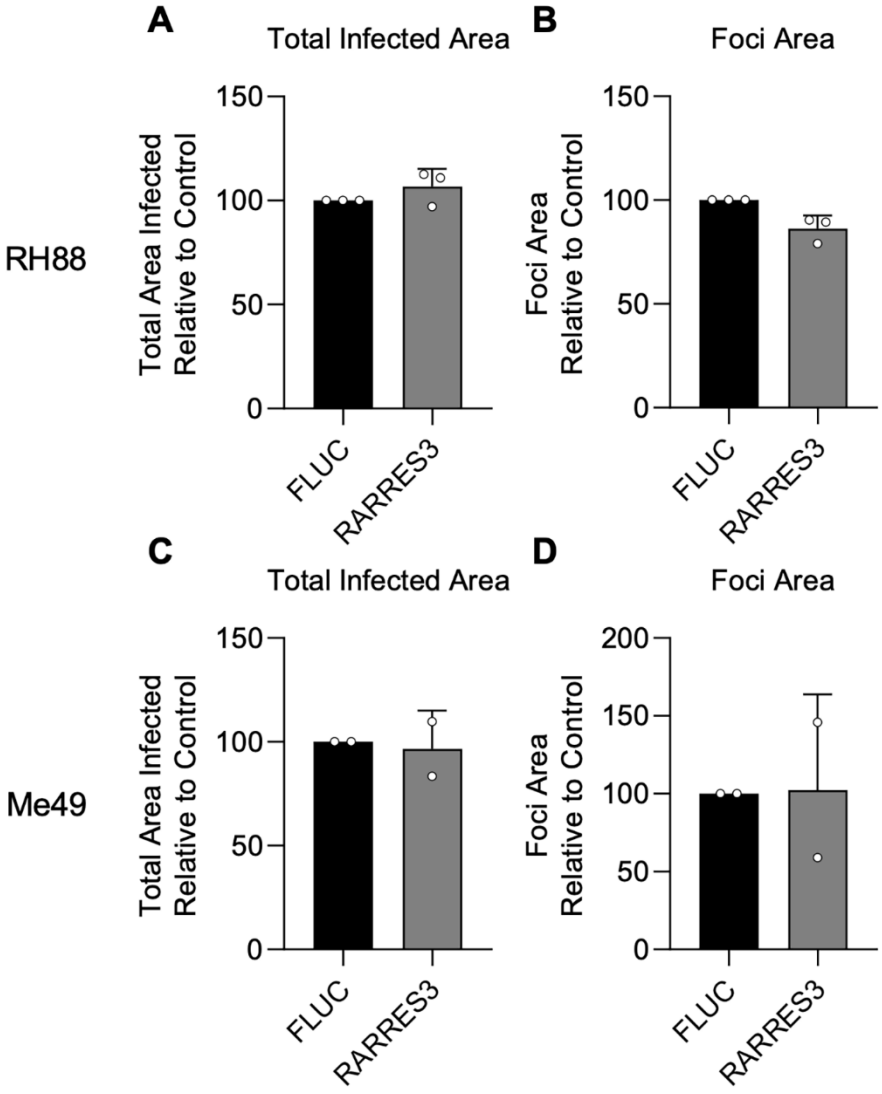

Supplemental Figure 1. RARRES3 does not restrict infection of Type I or II strains of *Toxoplasma gondii*. A549 cells were transduced with TRIP.RARRES3 and infected 72 h later with a type I strain expressing GFP (RH88-GFP) (A-B) or a type II strain expressing GFP (Me49-GFP) (C-D) for 4 d or 6 d respectively. Cells were fixed, stained with anti-GFP and anti-RFP antibodies, and imaged using a Cytation3 Imager. Average total infected area per well (A, C) and average area of infection foci (B, D) is shown. Data represent means ± standard deviation of two to three biological replicates conducted in technical triplicate. Statistical significance was determined using two-way ANOVA with Tukey's test for post-hoc analysis.

721

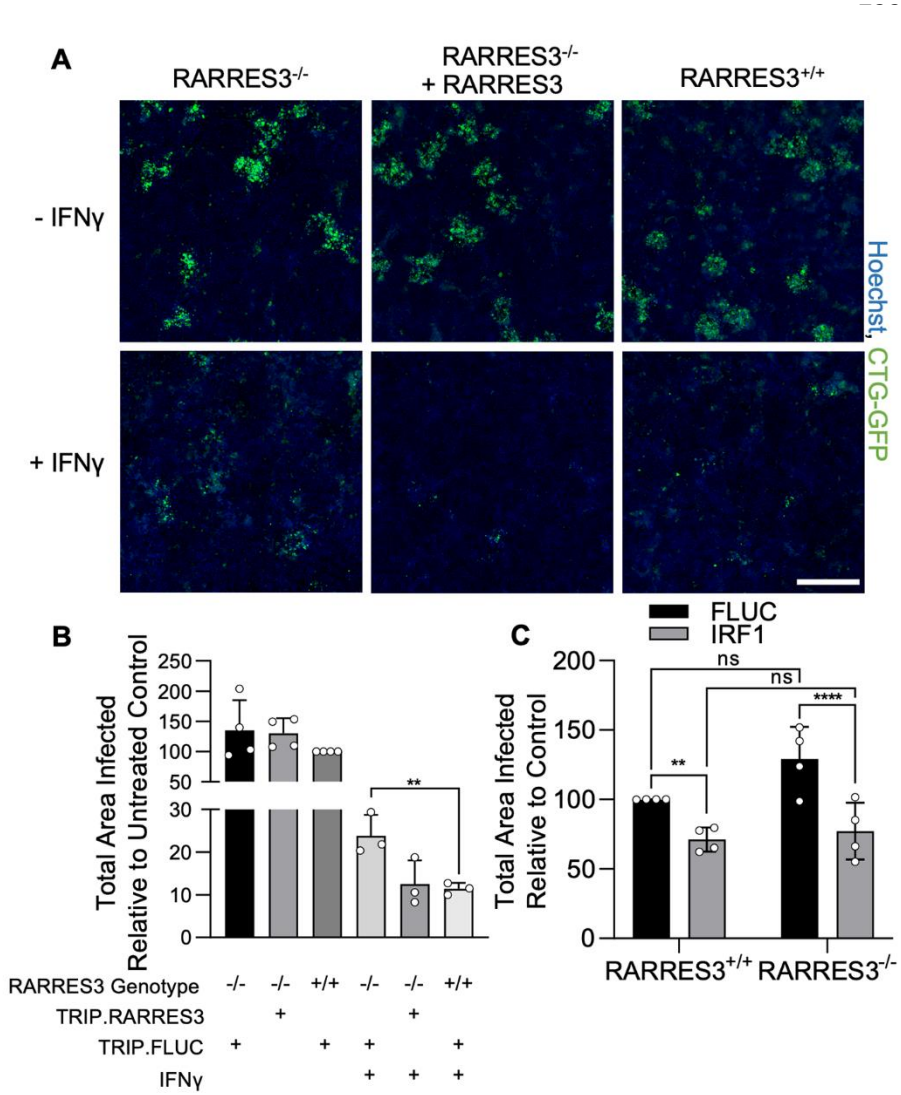

Figure 5. RARRES3 deficiency partially reverses IFNγ mediated restriction of *Toxoplasma* infection. RARRES3$^{-/-}$ A549s or wildtype cells transduced with a nontargeting CRISPR/Cas9 sgRNA were transduced with Cas9 resistant TRIP.RARRES3 or TRIP.FLUC as indicated. 72 hours later, cells were treated with or without 100 U/mL IFNγ for 24 h as indicated and subsequently infected with CTG-GFP for 96 h. Cells were harvested, stained with anti-GFP and anti-RFP antibodies, and imaged with a Cytation3 Imager. (A) Representative images and (B) quantitation are shown. Scale bar = 500 µm. (C) RARRES3$^{-/-}$ or RARRES3$^{+/+}$ A549 cells transduced with a nontargeting CRISPR/Cas9 control sgRNA were transduced with TRIP.FLUC or TRIP.IRF1 derived lentivirus. After 72 h, cells were infected with CTG-GFP for 96 h, harvested, stained with anti-GFP and anti-RFP antibodies, and imaged with a Cytation3 Imager. Average total infected area per well is shown. Data represent means ± standard deviation of four biological replicates conducted in technical triplicate. Statistical significance was determined using two-way ANOVA with Tukey's test for post-hoc analysis. ns $P > 0.05$, ** $P < 0.01$, **** $P < 0.0001$.

748

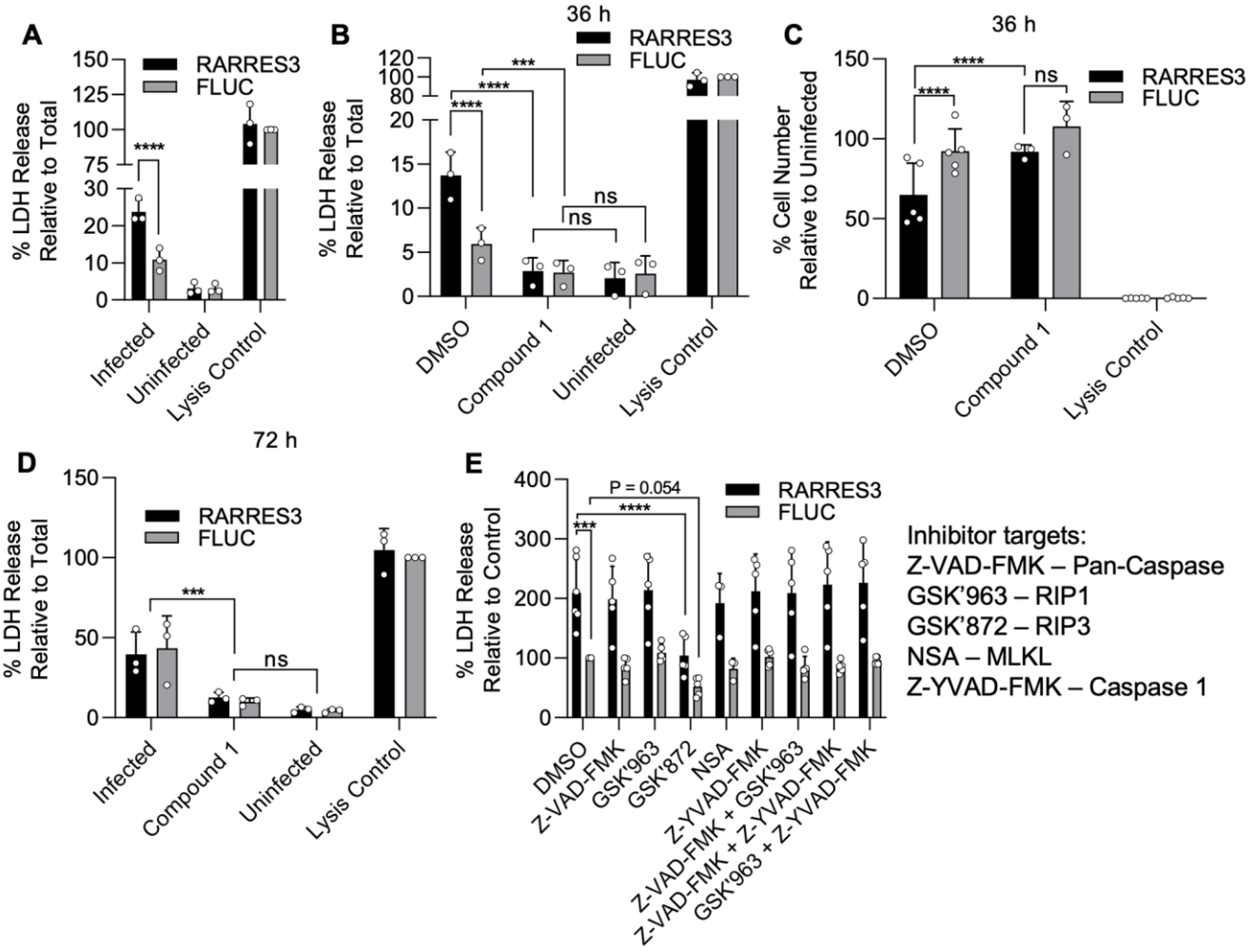

Figure 6. RARRES3 promotes premature egress of *T. gondii*. A549 cells were transduced with TRIP.RARRES3 or TRIP.FLUC control and infected 72 h later with CTG-GFP for 36 (A-C, E) or 72 (D) h. Cells were treated with the cell death inhibitors Z-VAD-FMK (50 µM), GSK'963 (1 µM), GSK'872 (5 µM), NSA (10 µM), or Z-YVAD-FMK (10 µM) as indicated during infection. (A, B, D, E) Cell supernatant was collected after infection and lactate dehydrogenase (LDH) activity was determined to measure cell lysis. As a control to measure maximal LDH release, cells were lysed before supernatant collection. (C) Cells were fixed, stained with anti-RFP and anti-GFP antibodies, and imaged with a Cytation3 Imager. Average cells per field are shown. Data represent the means ± standard deviation of three to five biological replicates conducted in technical duplicate. Statistical significance was determined using two-way ANOVA with Tukey's test for post-hoc analysis. ns $P > 0.05$, * $P \leq 0.05$, *** $P < 0.001$, **** $P < 0.0001$.

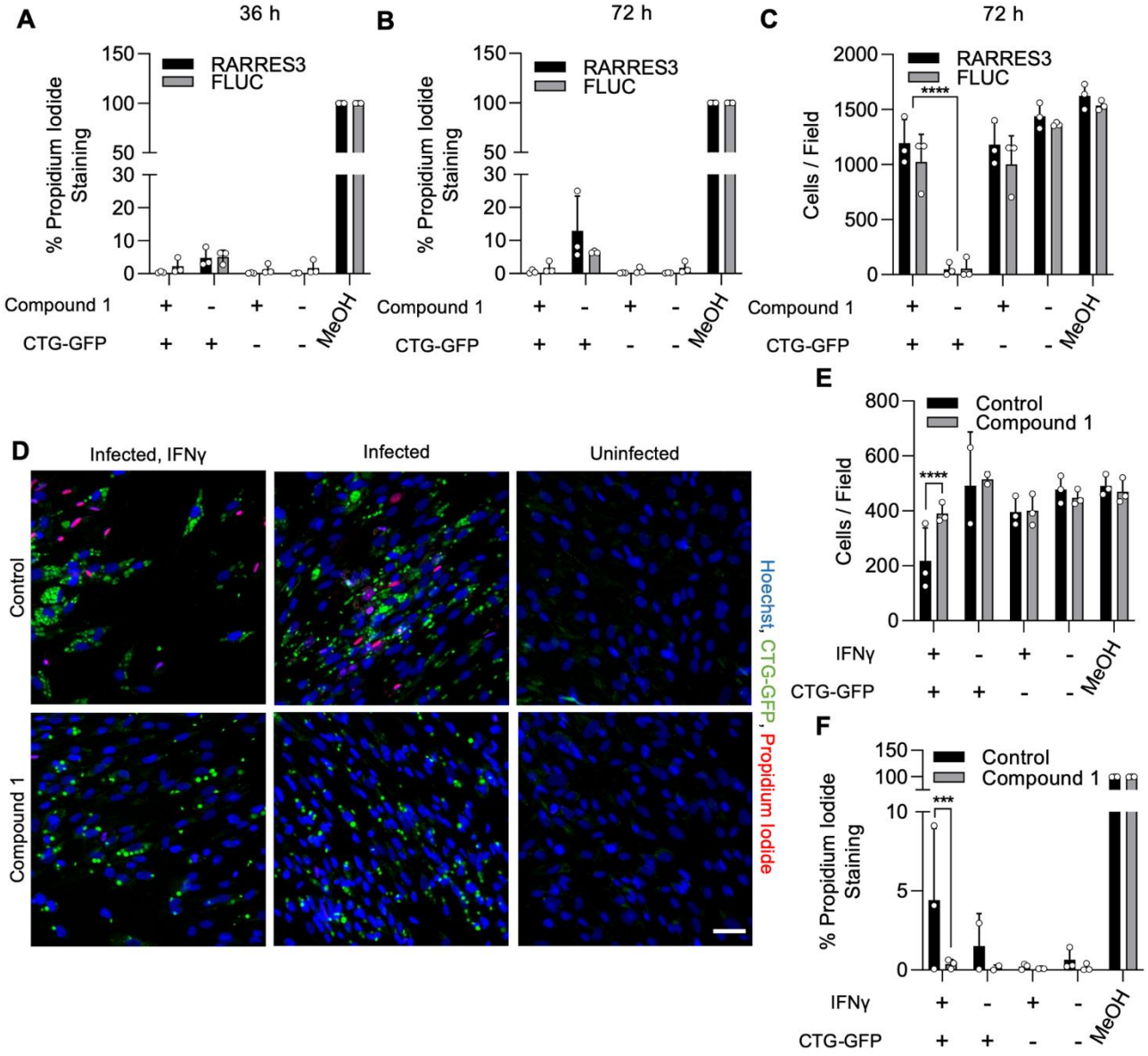

760
761 **Supplemental Figure 2. Compound 1 prevents host cell death during infection.** (A-C) A549 cells were transduced
762 with TRIP.RARRES3 or TRIP.FLUC control and infected 72 h later with CTG-GFP for 36 h (A) or 72 h (B-C). Cells were
763 stained with Hoechst 33342, propidium iodide, and imaged with a Cytation3 imager. As a positive control, cells were
764 permeabilized by treatment with methanol (MeOH) for 5 min prior to staining. The percentage of propidium iodide
765 staining cells (A, B) and average cell number per field (C) were determined. (D-F) HFF cells were pretreated with or
766 without IFNγ for 24 h and subsequently infected with CTG-GFP for 36 h. Cells were stained with Hoechst 33342,
767 propidium iodide, and imaged with a Cytation3 imager. As a positive control, cells were permeabilized by treatment
768 with methanol (MeOH) for 5 min prior to staining. (D) Representative images are shown. Scale bar = 50 µm. Average
769 cell number (E) and the percentage of propidium iodide staining cells (F) were determined. Data represent means ±
770 standard deviation of two or three biological replicates conducted in technical duplicate. Statistical significance was
771 determined using two-way ANOVA with Tukey's test for post-hoc analysis. *** *P < 0.001*, **** *P < 0.0001*.

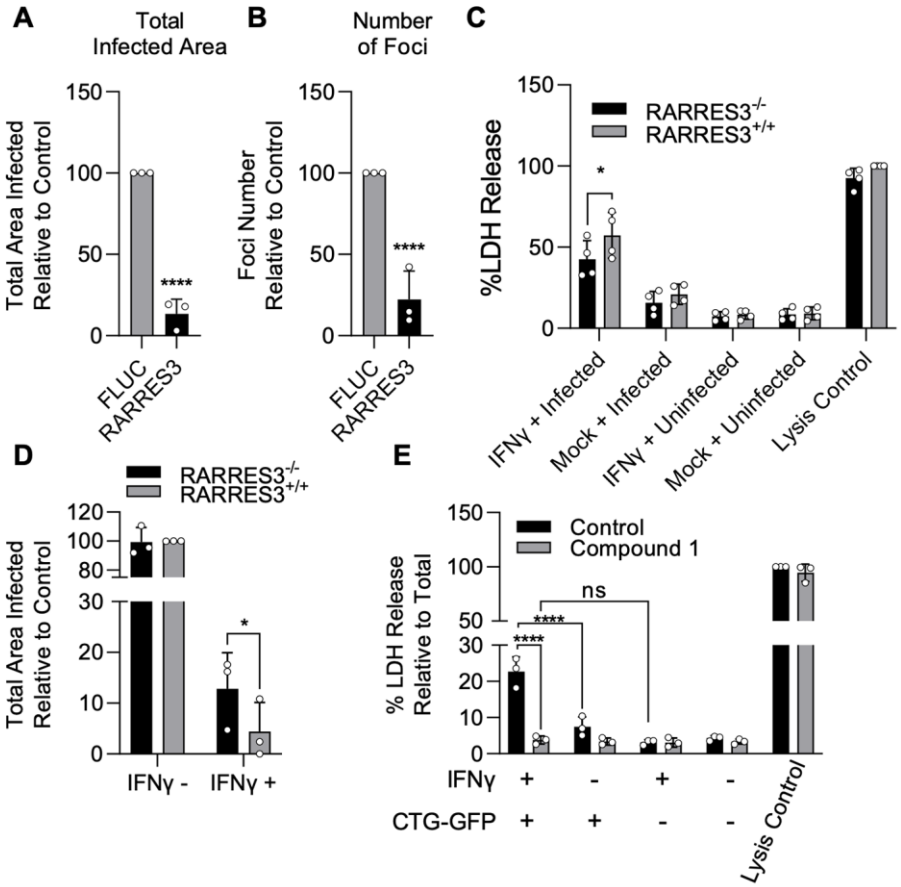

Figure 7. IFNγ -dependent host cell death during infection in HFFs is partially RARRES3 dependent. (A-B) HFF cells were transduced with TRIP.RARRES3 or TRIP.FLUC control and infected 72 h later with CTG-GFP for 96 h. Cells were fixed, stained with anti-GFP and anti-RFP antibodies, and imaged using a Cytation3 Imager. Total infected area per well (A) and average number of infection foci (B) is shown. (C-D) WT HFFs expressing a nontargeting sgRNA control or RARRES3 deficient HFFs were pretreated with or without 1000 U/mL IFNγ for 24 h. (C) Cells were infected with CTG-GFP for 36 h. Supernatant was collected and lactate dehydrogenase (LDH) activity was determined. As a control to measure maximal LDH release, cells were lysed before supernatant collection. (D) Cells were infected with CTG-GFP for 96 h. Samples were treated as in A. Total infected area per sample is shown. (E) HFFs were infected with CTG-GFP for 36 h in the presence or absence of 5 µM Compound 1. Supernatant was collected and LDH activity was determined. Data represent means ± standard deviation of three (A,B,D,E) or four (C) biological replicates conducted in technical duplicate (A,B,D,E) or singlet (C). Statistical significance was determined using two-way ANOVA with Tukey's test for post-hoc analysis. * $P \leq 0.05$, *** $P < 0.001$, **** $P < 0.0001$.

798 **Supplemental Table 1. List of primer sets used.**

799 **Dataset 1. Summary of over-expression screen in A549 cells.**

800 **Dataset 2. List of genes induced by IRF1 ectopic expression or IFNγ treatment in A549 cells.**

801 **Dataset 3. Comparison of genes induced by IRF1 or IFNγ with genes in the type II ISG screen library.**